Resolution of Undistorted Symmetric Immobile DNA Junctions by *Vaccinia* Topoisomerase I†

Shiping Liao,‡ Chengde Mao,§ Jens J. Birktoft,‡ Stewart Shuman,|| and Nadrian C. Seeman*,‡

Department of Chemistry, New York University, New York, New York 10003, Department of Chemistry, Purdue University, West Lafayette, Indiana 47907, and Molecular Biology Program, Sloan-Kettering Institute, New York, New York 10021

Received October 7, 2003; Revised Manuscript Received November 24, 2003

ABSTRACT: Holliday junctions are intermediates in genetic recombination. They consist of four strands of DNA that flank a branch point. In natural systems, their sequences have 2-fold (homologous) sequence symmetry. This symmetry enables the molecules to undergo an isomerization, known as branch migration, that relocates the site of the branch point. Branch migration leads to polydispersity, which makes it difficult to characterize the physical properties of the junction and the effects of the sequence context flanking the branch point. Previous studies have reported two symmetric junctions that do not branch migrate: one that is immobilized by coupling to an asymmetric junction in a double crossover context, and a second that is based on molecules containing 5′,5′ and 3′,3′ linkages. Both are flawed by distorting the structure of the symmetric junction from its natural conformation. Here, we report an undistorted symmetric immobile junction based on the use of DNA parallelogram structures. We have used a series of these junctions to characterize the junction resolution reaction catalyzed by *vaccinia* virus DNA topoisomerase. The resolution reaction entails cleavage and rejoining at CCCTT↓N recognition sites arrayed on opposing sides of the four-arm junction. We find that resolution is optimal when the scissile phosphodiester (Tp↓N) is located two nucleotides 5′ to the branch point on the helical strand. Covalent topoisomerase-DNA adducts are precursors to recombinant strands in all reactions, as expected. Kinetic analysis suggests a rate limiting step after the first-strand cleavage.

The Holliday (*1*) junction is the most prominent DNA intermediate in genetic recombination. It is known to be involved in site-specific recombination (*2*−*4*), and it is likely to be involved in homologous recombination (*5*). The involvement of the Holliday junction in recombination is illustrated in Figure 1. The first step, shown at the left of the drawing, is the formation of the branched intermediate (**II**) from two pieces of DNA containing homology (**I**). The branch point of the Holliday junction is flanked typically by regions of dyad (homologous) sequence symmetry; this symmetry enables the branch point to relocate through an isomerization known as branch migration (e.g., ref *6*). The product (**III**) of branch migration is illustrated in the step to the right of the formation. Proceeding to the right, the Holliday junction may undergo another conformational change, known as crossover isomerization. This rearrangement reverses the helical and crossover strands (**IV**), and it is known to be spontaneous (*7*). The junctions then may be cleaved (**V**) by resolvases, such as endonuclease VII (*8*) or RuvC (*9*). The nicked linear products of endonucleolytic resolution can then be sealed by DNA ligase (**VI**). *Vaccinia* virus topoisomerase I (VTopo I) can perform both the cleavage and ligation steps on Holliday junctions that contain its CCCTT recognition site (*10*).

The symmetry that enables branch migration makes it difficult to study the features of Holliday junctions. For example, it is difficult to characterize the crossover preferences of Holliday junctions when the sequence at the branch point is not fixed. To overcome this problem, a symmetric immobile junction (SIJ) (*11*) based on double crossover (DX) molecules (*12*) was introduced in 1993. In this system, two junctions are separated by one or one-and-a-half helical turns. One of these junctions is flanked by a symmetric sequence, but the other is immobile because it is not flanked by a symmetric sequence. At this short separation, the migration of the two junctions is closely coupled. Consequently, the immobility of the asymmetric junction translates into immobility for the symmetric junction because its migration would alter significantly the twist in the intervening region. These SIJ molecules have been used to characterize the thermodynamics of crossover isomerizations (*13*) and of branch migratory minima (*14*) associated with symmetric sequences. We have also used them to establish the feasibility of branch migration in antiparallel junctions (*15*) and to characterize the location of the branch point when it is cleaved by RuvC (*16*). The key flaw involving this first kind of SIJ molecule (SIJ1K)[1] is that its interdomain angle is constrained to be exactly antiparallel, unlike the angles

† This research has been supported by Grants GM-29554 from the National Institute of General Medical Sciences and N00014-98-1-0093 from the Office of Naval Research; by Grants DMI-0210844, EIA-0086015, DMR-01138790, and CTS-0103002 from the National Science Foundation and F30602-01-2-0561 from DARPA/AFSOR to N.C.S.; by NIH Grant GM46330 to S.S.; and by NSF Grant EIA-0323452 to C.M.

* To whom correspondence should be addressed. Phone: (212) 998-8395. Fax: (212) 260-7905. E-mail: ned.seeman@nyu.edu.

‡ New York University.

§ Purdue University.

|| Sloan-Kettering Institute.

10.1021/bi0358061 CCC: $27.50
Published on Web 01/24/2004

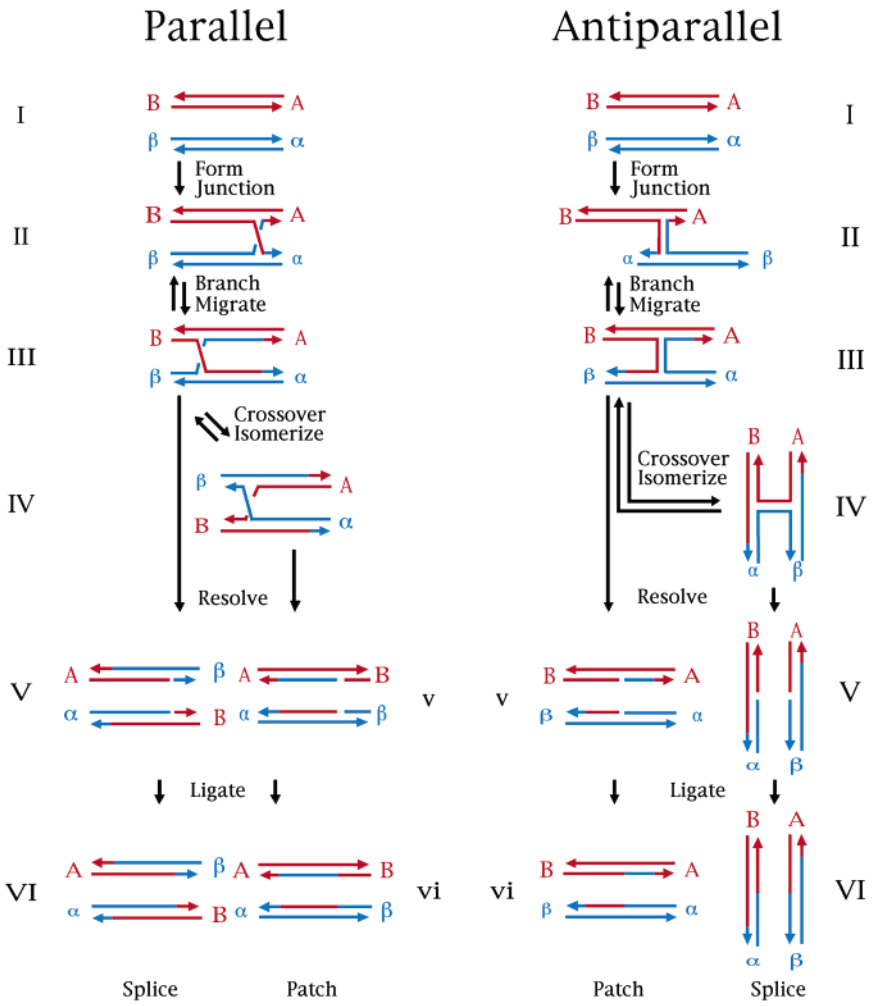

FIGURE 1: Formation and resolution of the Holliday structure in genetic recombination. The process is illustrated both in the commonly shown parallel conformation and also in the antiparallel conformation, suggested by physical data; it proceeds from the left to the right. Each of the possible stages is labeled with capital or small Roman numerals. In the first stage, I, two homologous double helices of DNA align with each other. The two strands of each duplex are indicated by the two pairs of lines terminated by half arrows, which indicate the 3′ ends of the strands. Strands are distinguished by their colors, red and blue. Each of these two homologous regions carries a flanking marker, A and B in the strands on the left and α and *β* on the right. After the first step, the homologous pairs have formed a Holliday intermediate, **II**, by exchanging strands. Note that the two crossover strands are composite strands with both a red and a blue portion formed through any of a number of possible mechanisms. The homologous 2-fold sequence symmetry of this structure permits it to undergo the iterative isomerization process, branch migration; movement in the direction indicated results in structure **III**. The Holliday intermediate may or may not undergo the crossover isomerization process to produce structure **IV**, in which the crossover and noncrossover strands are switched. Although indicated as separate, the crossover isomerization process could be a feature of branch migration (*8*). If crossover isomerization occurs an odd number of times, resolution by cleavage of the crossover strands yields structure **V**, but structure **v** results if crossover isomerization occurs an even number of times (including 0) before cleavage. Ligation of **v** generates a patch recombinant, **vi**; this is a pair of linear duplex DNA molecules containing heteroduplex DNA because of branch migration but that have retained the same flanking markers. Ligation of **VI** yields splice recombinant molecules that have exchanged flanking markers. Cleavage of the noncrossover strands reverses the products, so that **V** would yield a patch recombinant and **v** would yield a splice recombinant.

measured in solution (*17*, *18*), on surfaces (*19*), or in the most representative crystals (*20*), which are 40−60° from that orientation. As a substrate, a further limitation of SIJ1K molecules is that recognition sites may be occluded in the molecule, which is known to be quite rigid (*21*, *22*).

Recently, we have described a second kind of SIJ molecule (SIJ2K), based on Bowtie junctions (*23*). Bowtie junctions (*24*) are Holliday-like junctions containing 5′,5′ and 3′,3′ linkages on their crossover strands. They are similar to conventional Holliday junctions in that they stack their four arms to produce two helical domains. However, they differ from conventional junctions in that the orientation of these helical domains changes by about 50°, so that they are in the parallel rather than antiparallel range of conformations (*24*, *25*). The unusual linkages confer immobility on these junctions, even if the sequence flanking the junction is symmetric, because branch migration would entail replacing antiparallel nucleotide pairs with parallel pairs, an arrangement unlikely to be favored (*26*). SIJ2K molecules provide

[1] Abbreviations: Bowtie junction, Holliday junction analogue containing 5′,5′ and 3′,3′ linkages in its crossover strands; BSA, bovine serum albumin; DTT, dithiothreitol; EDTA, ethylenediaminetetraacetic acid; SI, symmetric immobile; SIJ, symmetric immobile junction; SIJ1K, symmetric immobile junction of the first kind; SIJ2K, symmetric immobile junction of the second kind; SIJ3K, symmetric immobile junction of the third kind; TAEMg, solution containing 40 mM Tris, pH 8.0, 20 mM acetic acid, 2 mM EDTA and 12.5 mM magnesium acetate; TBE, solution containing 100 mM Tris, pH 8.3, 89 mM boric acid and 2 mM EDTA; VTopo I, *vaccinia* virus topoisomerase I.

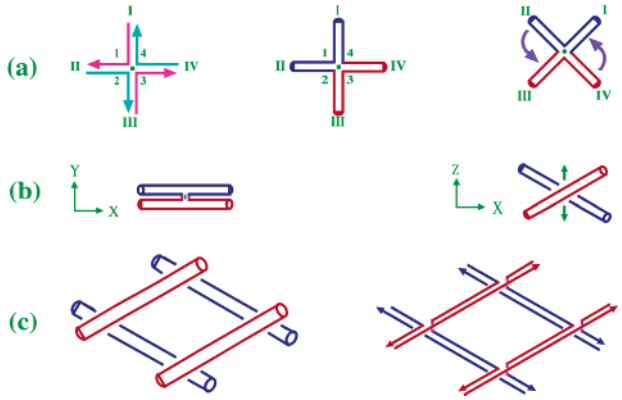

FIGURE 2: Schematic representations of the Holliday junction and its use as a parallelogram component. (a) Representations of the Holliday junction. The left panel shows the Holliday junction as four strands, in two homologous pairs, as represented by the colors; the double helical arms are labeled with Roman numerals. The middle panel represents the same structure but emphasizing its helical structure; here, adjacent helices are colored the same. The right panel rotates the molecule and indicates with curved arrows the folding of the helices into a stacked structure. (b) The stacked structure. The left panel shows a view down the dyad axis of the Holliday junction; the dyad replaces the nominal 4-fold axis indicated in panel a. The dyad axis is indicated by the small lens-shaped figure. The upper helical domain is rotated 30° about the vertical so that its right end penetrates the page, and the lower helical domain is rotated 30° about the vertical so that its left end penetrates the page. The *X* and *Y* axes of a right-handed coordinate system are shown to help orient the reader. The right panel shows a view with the dyad axis vertical. The molecule has been rotated 90° about the *X* axis of the coordinate system. The dyad axis is indicated by the double arrows. (c) The Rhombus-like motif and its strand structure. In the left part, four molecules, in the orientation of the right part of panel b, are combined. The red helices are about 2 nm closer to the reader than the blue helices. The strand structure of a molecule with an exact number of turns between crossover points is shown in the right panel. Arrowheads indicate 3′ ends of strands. As in the left panel, the parallel helices are drawn in identical colors, red and blue; note that some strands contain both red and blue segments.

different types of constraints from the SIJ1K molecules, leading both to advantages and disadvantages: on the positive side, there is no enforcement of planarity on the double helical domains; on the negative side, the angle between helical domains is different from that seen for conventional junctions, and the linkage in the crossover strands is unnatural. SIJ2K molecules have been used to demonstrate communication between the subunits of RuvC resolvase (*23*).

In work with a different focus, we have reported the construction of crystalline two-dimensional Holliday junction parallelogram arrays (*19*). The components of these arrays are shown in Figure 2. Figure 2a,b shows how the cruciform representation of the Holliday junction folds to produce the well-known twisted antiparallel structure (*27*, *28*). Four of these Holliday junctions can be combined to produce a parallelogram-like structure consisting of four helical domains. The two red edges of the parallelogram (in this case, a rhombus) in Figure 2c are about 2 nm closer to the reader than the two blue edges. The blue edges are connected to the red edges by the Holliday crossover. We have used parallelogram arrays to measure the angle between the domains of an immobile junction (*19*), to characterize features of the Bowtie junction (*25*), as the basis for suggested fractal patterns (*29*, *30*), and to demonstrate that the angle between the helical domains of a particular symmetric junction (*20*) is different from the usual angle noted in immobile junctions (*31*). It is important to realize that there is no stress on the junctions, so long as the helical domains between crossovers contain integral numbers of either whole- or half-turns of double helical DNA.

The individual parallelogram is potentially a system that can be used to apply constraints, similar to the DX molecule. This notion suggests that the torsional rigidity of the DNA double helical domains within a small parallelogram might be used to produce an undistorted symmetric immobile junction. Using the same principle as in the SIJ1K molecule (i.e., that immobile junctions can immobilize symmetric junctions), an undistorted symmetric immobile junction ought to result from a parallelogram with short edges containing three immobile junctions and one symmetric junction. We have tested this notion experimentally, and below we demonstrate that it is correct; thus, we have produced a third kind of symmetric immobile junction (SIJ3K) that is undistorted.

We have applied this system to the enzymatic production of recombinant products by *vaccinia* virus DNA topoisomerase I. VTopo I exemplifies the type IB topoisomerase enzymes, which cleave and rejoin one strand of the DNA duplex via a covalent DNA-(-3′-phosphotyrosyl)-enzyme intermediate. VTopo I is distinguished by its site-specificity in DNA transesterification. VTopo I binds and incises duplex DNA at a pentapyrimidine target sequence 5′-(T/C)CCTT↓ (*32*). VTopo I is mechanistically and structurally related to the tyrosine recombinase enzyme family (*33*−*35*); the tyrosine recombinases catalyze conservative DNA rearrangements by forming and then resolving Holliday junctions. We showed previously that VTopo I catalyzes the resolution of a four-arm Holliday junction that contained two CCCTT cleavage sites for VTopo I situated on opposing strands within a 10-bp mobile homologous core at the crossover. VTopo I catalyzed rapid and efficient resolution of this junction (80% of input DNA resolved) via strand cleavage and conservative strand transfer within the CCCTT-containing 10-bp core (*10*). Modifications to the mobile core that progressively limited branch migration diminished (8-bp mobile junction), and then abolished (6-bp mobile junction), the resolvase activity of VTopoI (*36*). These studies suggested that VTopo I is unable simultaneously to transesterify two CCCTT↓ sites at the junction unless they are retracted into the junction arms and the scissile phosphates are separated by a spacer DNA. However, a problem in interpreting these data is that the mobile junctions can undergo branch migration and spontaneous crossover isomerization, so that neither the positions of the crossover relative to the scissile phosphates on the Topo-resolvable junctions nor the location of the scissile phosphate on the helical versus crossover strands can be surmised.

Here we use symmetric immobile junctions of the SIJ3K type to analyze systematically how the positioning of the scissile phosphates on the crossover or noncrossover strands and their spacing from the junction crossover influence the resolvase activity of VTopo I. We find that resolution is optimal when the scissile phosphates are located two nucleotides 5′ to the crossover point on the helical strand of the junction.

MATERIALS AND METHODS

Synthesis and Purification of DNA. All DNA molecules used in this study were synthesized on an Applied Biosystems 380B automatic DNA synthesizer, removed from the support, and deprotected using routine phosphoramidite procedures (*37*). All strands were purified by polyacrylamide gel electrophoresis.

Formation of Undistorted Symmetric Immobile Junction Molecules. The component strands of the undistorted symmetric immobile junction were dissolved to a concentration of 1 μM in a solution containing 40 mM Tris, pH 8.0, 20 mM acetic acid, 2 mM EDTA, and 12.5 mM magnesium acetate (TAEMg), and the mixtures were cooled slowly from 90 to 4 °C.

Hydroxyl Radical Autofootprinting Analysis. Individual strands of the molecules were radioactively labeled and were additionally gel purified from a 14% denaturing polyacrylamide gel. Each of the labeled strands (approximately 4 pmol in TAEMg) was annealed to a 4-fold excess of the unlabeled complementary strand, or it was annealed to the complex, as described previously, or it was left untreated as a control, or it was treated with sequencing reagents (*38*) for a sizing ladder. Hydroxyl radical cleavage of the samples took place at 4 °C for 100 s (*39*), with modifications noted by Churchill et al. (*40*). The reaction was stopped by addition of thiourea. The samples were ethanol precipitated, dried, dissolved in a formamide/dye mixture, and loaded directly onto a 14% polyacrylamide sequencing gel containing 8.3 M urea. Autoradiograms were quantitated using a Storm 860 Gel and Blot Imaging System (Amersham Pharmacia Biotech, Piscataway, NJ).

Enzymatic Reactions. (*A) Kinase Labeling.* Two pmol of an individual strand of DNA was dissolved in 10 μL of a solution containing 50 mM Tris·HCl, pH 7.6, 20 μM spermidine, 10 mM $MgCl_2$, 15 mM dithiothreitol (DTT), and 0.2 mg/mL nuclease free bovine serum albumin (BSA) (US Biochemical) and mixed with 1 μL of 1.25 mM γ-^{32}P-ATP (10 μCi/μL) and 3 units of T4 polynucleotide kinase (USB) for 2 h at 37 °C. The reaction was stopped by phenol extraction, and DNA was recovered by ethanol precipitation.

(B) Topoisomerase Treatment. Vaccinia virus topoisomerase I was prepared as described previously (*41*). Reaction mixtures (20 μL) containing 20 mM Tris-HCl (pH 8.0), 12.5 mM Mg^{2+}, 2 pmol SIJ3K complex, and 20 pmol of *vaccinia* topoisomerase were incubated at 37 °C for 30 min. The reaction was terminated by adjusting the solution to 0.2% SDS and 0.5 mg/mL proteinase K. After incubation at 37 °C for 1 h, the DNA products were extracted successively with phenol, phenol/chloroform, and chloroform. For nondenaturing gel analysis, the aqueous phase was removed and adjusted to 5% glycerol, prior to electrophoresis. For denaturing gel analysis, the proteinase K-treated products of the resolution reaction were precipitated with ethanol, resuspended in formamide, heat-denatured, and then electrophoresed.

Denaturing Polyacrylamide Gel Electrophoresis. These gels contained 8.3 M urea and were run at 55 °C. Gels contained 6−20% acrylamide (19:1, acrylamide/bisacrylamide). The running buffer consisted of 100 mM Tris, pH 8.3, 89 mM boric acid, 2 mM EDTA (TBE). The sample buffer consisted of 10 mM NaOH, 1 mM EDTA, and 90% formamide and contained 0.1% Xylene Cyanol FF tracking dye. Gels were run on an IBI Model STS 45 electrophoresis unit at 70 W (50 v/cm), constant power and dried onto Whatman 3MM paper, and the distribution of each species was quantitated using a Storm 860 Gel and Blot Imaging System (Amersham Pharmacia Biotech, Piscataway, NJ).

Nondenaturing Polyacrylamide Gel Electrophoresis. Gels contained 6 or 8% acrylamide (19:1, acrylamide/bisacrylamide). DNA was suspended in 10−25 μL of TAEMg, and the strands were annealed as described previously. Samples were then brought to a final volume of 20 μL and a concentration of 1 μM DNA, with a solution containing TAEMg, 50% glycerol, and 0.02% each of Bromophenol Blue and Xylene Cyanol FF tracking dyes. Gels were run on a Hoefer SE-600 gel electrophoresis unit at 11 V/cm at 4 °C and stained with Stainsall dye (Aldrich).

Docking Protocols. (A) Holliday Junction DNA. The DNA Holliday junction was derived from the 2.1 Å crystal structure of a 20 base-pair Holliday junction (*20*). The interhelical angle was changed from 41° observed in the crystal structure to ~60° by rotation about the bonds flanking the central phosphate in the two crossing strands. The four arms of the junction were extended to a total length of 15 base pairs maintaining the B-DNA conformation, and the sequence was adjusted to that of the H2 design (see below). No solvent molecules were incorporated in the model.

(B) VTopo I. The published structure of the catalytic domain of VTopo I (*35*) has been reported to be homologous to that of *Cre*-recombinase (*35*, *36*) sharing the same catalytic residues. Importantly, these residues are located on corresponding elements of secondary structure. The structure of VTopo I is that of the unliganded form of the enzyme, whereas several *Cre*-DNA cocrystal structures have been determined, including that of a covalent intermediate (*35*). The structure of VTopo I was first aligned with that of the *Cre*-DNA complex (PDB: 4CRX) using the protein and only the part of the DNA from the 5′ end up to the site of the covalent attachment to the *Cre* active site tyrosine, Tyr324 (Tyr274 in VTopo I). The proteins were first aligned as suggested in ref *34*, and then the structure of VTopo I was adjusted such that homologous secondary structural elements in VTopo I and *Cre* were aligned with each other. Other segments in VTopo I were adjusted accordingly, to maintain structural integrity. A B-DNA helix was superimposed on top of the DNA bound to *Cre*, aligning it with the segment from the 5′ end to the phosphate bound to Tyr324 of *Cre*. This brought the catalytic and binding site residues in VTopo I into functional proximity to the fitted DNA; in particular, this superposition placed Tyr274 adjacent to the phosphate (named P*) at the cleavage site, with which it forms a covalent link. The [H2] − [VTopo I − DNA] complex was then fitted to the Holliday junction DNA by aligning P* to the P_{H2} phosphate, P^*_{n-1} to P_{H-1}, P^*_{n-2} to P_{H-2}, P^*_{n-3} to P_{H-3}, etc. An identical procedure was followed for the site related by 2-fold symmetry on the other domain of the junction. The models of the other [H-site] − [VTopo I − DNA] complexes were generated in a similar manner. The N-terminal domain of VTopo I was not included in the modeling; although its structure is known, no direct knowledge of its binding mode has been noted. If it is assumed that the N-terminal domain binds as suggested by Cheng et al. (*33*), no interference appears to take place at site H2 (see

below for nomenclature), while increasing contacts with the opposite double helix seem to be the case for binding to H1 and H0 and severe contacts at site C2. The graphics work was conducted with the Turbo-Frodo program (*42*). Figures were created with the Ribbons program (*43*).

RESULTS

Sequence and Molecular Design of the SIJ3K Molecules. The basis for the design of the immobile junctions in the parallelogram is the well-characterized J1 junction (*44*, *45*), used in previous studies. Three junctions of the parallelogram are composed of the J1 sequence, and the fourth junction consists of a symmetric sequence flanking the crossover point that includes the *vaccinia* topoisomerase recognition sequence, CCCTT. The first SIJ3K molecule that we made contained 10 nucleotide pairs (~1 turn) per edge. However, to test a range of sites containing CCCTT, it is more convenient to use a molecule with slightly longer edges, so the molecules we used contained 16 nucleotide pairs per edge, ~1.5 turns. We have been able to show by hydroxyl radical autofootprinting that the symmetric junction in this molecule is also immobile (see below). The sequences have been selected by using the program SEQUIN (*46*). The sequence of the entire SIJ3K molecule and the junction-flanking sequence variants used are shown in Figure 3; the symmetric immobile site is labeled **SI**. The two arms containing the 5′ ends of strands 2 and 4 are intentionally of different lengths; this difference allows us to show that the recombination event catalyzed by VTopo I has occurred.

We have previously used SIJ1K molecules to determine the preferred site of RuvC cleavage of branched junctions (*16*). Such a determination entails a search over the positions available to the enzyme. Here, we have produced 10 different SIJ3K molecules. We have placed the final T of the CCCTT recognition sequence 0, 1, 2, 3, and 4 nucleotides 5′ to the crossover point on either the helical (H) or the crossover (C) strand. These variants are denoted as H0 through H4 and C0 through C4, respectively. The use of J1 junctions at the immobile sites enables us to know which strand will be the crossover strand and which will be the helical strand (*40*). It is known that VTopo I is capable of cleaving 5′ to the junction (*36*).

Molecular Assembly. We have used nondenaturing gel electrophoresis to characterize the assembly of many unusual DNA motifs in the past (e.g., ref *12*). A single band with mobility in the vicinity of a linear marker containing a similar number of nucleotides is taken to indicate the stability of the motif. Thus, neither breakdown products nor multimers can be evident in the lane. Figure 4 shows such a gel for one of the parallelograms produced, H2. The band corresponding to the complete parallelogram is shown in lane 2, and a series of incomplete complexes are shown to its right. There are 344 nucleotides in the parallelogram, and the molecule migrates in the range of 440−460 nucleotides of linear duplex DNA; this is not an unusual difference, given the different shape, topology, and surface area of the parallelogram. The absence of molecular dimers or breakdown products attests to the stability and the monodisperse nature of the parallelogram complex.

Hydroxyl Radical Autofootprinting. Hydroxyl radical autofootprinting is a biochemical tool that has been used for the preliminary structural characterization of a variety of unusual DNA motifs (*47*), particularly branched junctions

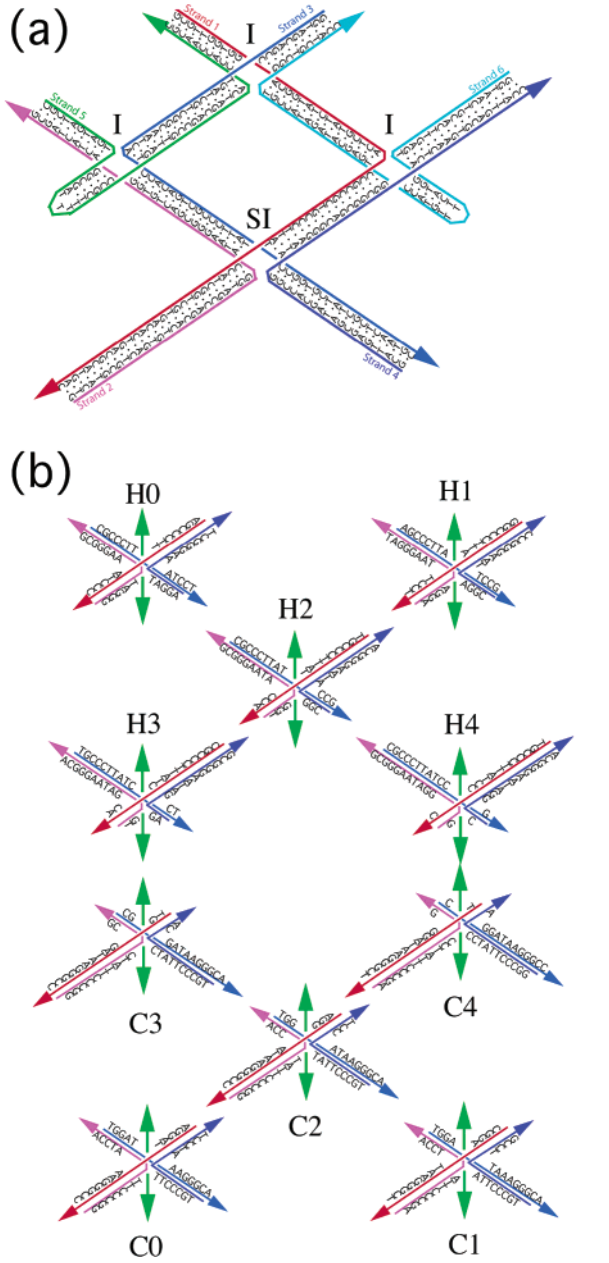

FIGURE 3: Sequences of the SIJ3K molecules used in this work. (a) The sequence of the whole parallelogram. Two pairs of the eight strands shown in Figure 2 have been fused for convenience through the use of hairpin loops, leaving six strands in the molecule. There are 16 nucleotide pairs between junctions, corresponding to 1.5 turns of DNA, and the three immobile junctions (top, left and right, indicated by **I**) are flanked by J1 (*44*, *45*) junctions. The symmetric immobile junction (labeled **SI**) is at the bottom, where strands 1 and 3 are its helical strands, and strands 2 and 4 are its crossover strands. Note that the external double helix formed by strands 1 and 2 is longer than the external double helix from by strands 3 and 4; this enables us to follow the progress of the recombination reaction catalyzed by VTopo I. (b) The sequences flanking the symmetric junction in each system. The five molecules labeled H0···H4 contain the recognition sequence, CCCTT, on the helical strands, zero to four nucleotides 5′ to the junction, respectively, within the body of the rhombus. The five molecules labeled C0···C4 contain the recognition sequence on the crossover strands zero to four nucleotides 5′ to the junction, respectively, now external to the rhombus. Note that the molecule shown in panel a corresponds to the H2 molecule.

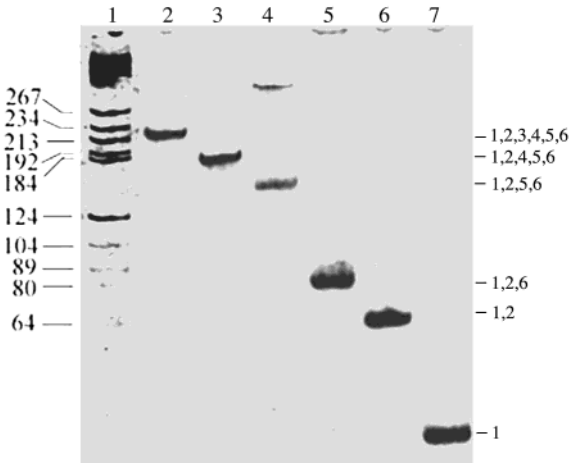

FIGURE 4: Nondenaturing gel of H2 parallelogram assembly. The image shows an 8% polyacrylamide gel run at 4 °C. Lane 1 contains a Hae III digested pBR322 marker. Lane 2 contains the target complex, an equimolar mix of strands 1−6. The lanes to the right show partial complexes: lane 3 contains strands 1, 2, 4, 5, and 6; lane 4 contains strands 1, 2, 5, and 6; lane 5 contains strands 1, 2, and 6; lane 6 contains strands 1 and 2; and lane 7 contains single strand 1. The multimer seen in lane 4 is the consequence of the unpaired nucleotides in this partial complex.

(*40*), SIJ1K molecules (*11*), and SIJ2K molecules (*23*). The experiment compares the quantitative hydroxyl radical cleavage pattern of each strand paired with its duplex complement to the pattern of the same strand complexed in the unusual motif. The duplex pattern serves to control for sequence effects and provides a baseline of known structure with which to compare the pattern in the unusual motif. If the cleavage pattern of the strand in the two complexes is the same, the inference is that the strand has adopted a helical structure in the unusual motif. The nucleotides flanking crossover points characteristically evince protection from cleavage, relative to the double helical control (*40*). For SIJ molecules, the key point is that the major sites of protection should be limited to the nucleotides flanking the target position of the symmetric junction. If the junction is not immobile, protection will be dispersed over a greater number of residues, or may even be unobservable, if the signal is diluted over a large range of nucleotides (*11*, *23*).

Figure 5 illustrates the hydroxyl radical autofootprinting analysis of the SIJ3K molecule at the symmetric junction. The pattern for each strand in the junction is compared with its pattern in a double helix. Figure 5a contains the autofootprinting pattern for the SI-position of a conventional immobile parallelogram with two turns of DNA between the crossover points; the extent of protection seen is characteristic of an immobile junction (*40*). Figure 5b shows the autofootprinting pattern of the symmetric junction in the parallelogram, which is similar to the pattern in Figure 5a: clear protection relative to duplex is visible at the nucleotides flanking the symmetric junction crossover points on strands 2 and 4. Thus, strands 2 and 4 are the crossover strands of this molecule, in accord with the design. This notion is supported by the absence of strong protection on strands 1 and 3, which are expected to be the helical strands of this junction. Very weak protection is also visible a few nucle-

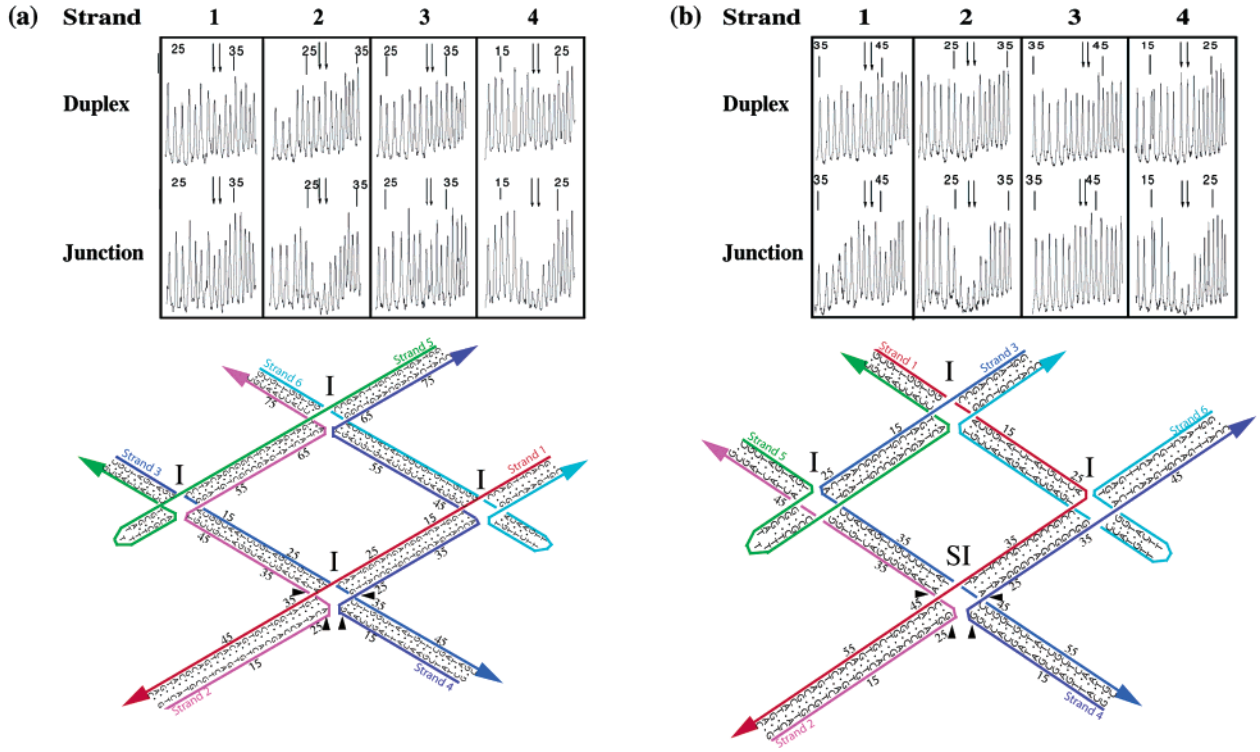

FIGURE 5: Hydroxyl radical autofootprinting of control (a) and SIJ3K (b) parallelograms. The data represent scans quantitating the cleavage by hydroxyl radicals of strands flanking the SI site junction. The strand in a double helical context (labeled Duplex) is used as a control with which to compare the pattern of the strand in the symmetric immobile junction (labeled Junction). The labeled strand is indicated above the pattern. The nominal position of the crossover point is indicated by two vertical arrows. The pattern of the control junction in panel a shows characteristic protection on the crossover strands (2 and 4), whereas the duplex and junction evince similar patterns in the helical strands (1 and 3). The pattern of the SIJ3K molecule is similar to the pattern of the control junction, indicating that it is immobile. The prominent features of the protection pattern are summarized on a schematic drawing below the cleavage data, where the immobile and symmetric immobile junctions are indicated by the convention of Figure 3.

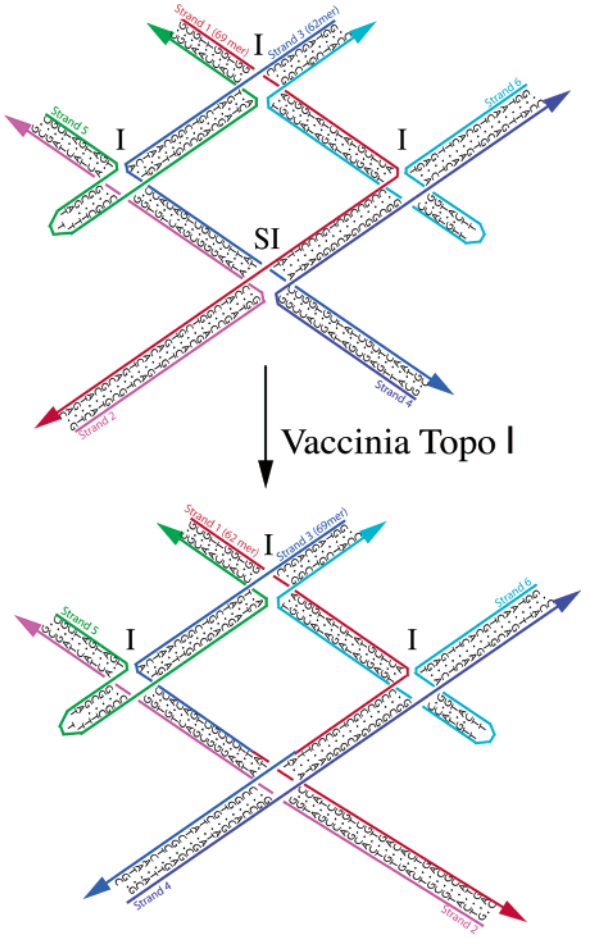

FIGURE 6: Reaction catalyzed by *vaccinia* virus topoisomerase I. The H2 molecule is shown in the top panel. The immobile and substrate symmetric immobile junctions are indicated by the convention of Figure 3. The strands are numbered, and the lengths of strands 1 (69 nucleotides) and 3 (62 nucleotides) are indicated. The bottom panel shows the product of the reaction, where the junction has been replaced by two double helices. Note that the two strands involved in the exchange have reversed sizes: strand 1 is now 62 nucleotides in length, and strand 3 now contains 69 nucleotides.

otides 3′ to the crossover point on the noncrossover strands, as seen previously (*40*) for junctions with this structure.

Recombination of SIJ3K Molecules by VTopo I. VTopo I is known to cleave and religate the strands of Holliday junctions (*10*). Figure 6 is a schematic diagram that illustrates the nature of this recombination event on the H2 SIJ3K molecule. The upper panel shows the substrate molecule; the symmetric Holliday junction is indicated by the symbol **SI**. The exchange will occur between the helical strands for this molecule. These are the 69-nucleotide strand 1 (red) and the 62-nucleotide strand 3 (royal blue). The lower panel shows the products of the recombination reaction. The reaction for this species has occurred two nucleotides 5′ to the junction point, so that strand 1 is now a 62-nucleotide red−blue strand, and strand 3 is now a 69-nucleotide blue−red strand. Note that the junction has been resolved, and the products in the lower part of the molecule are now two double helices.

Figure 7 shows a nondenaturing gel demonstrating that topoisomerase treatment leads to the appearance of a novel product with altered native mobility. For consistency, we show data throughout for the H2 system; analogous data have

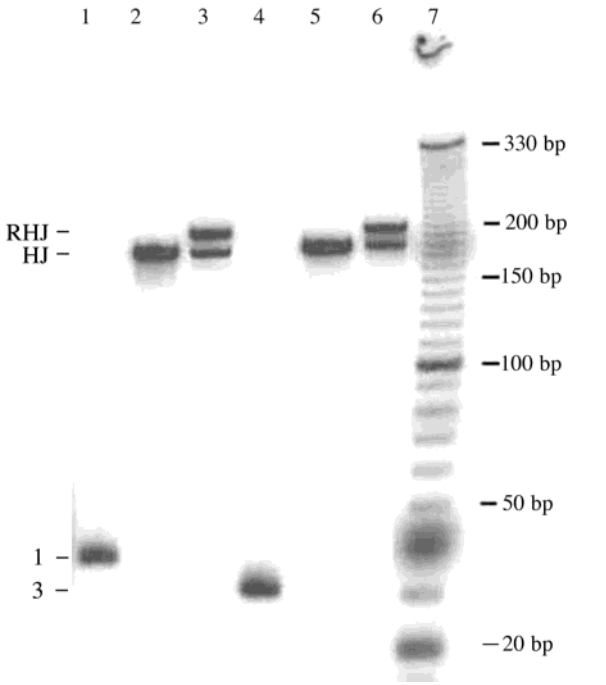

FIGURE 7: Nondenaturing gel examining the reaction catalyzed by *vaccinia* virus topoisomerase I. A 6% polyacrylamide gel autoradiogram of the H2 complex and its components is shown. Lane 7 contains a 10-bp marker ladder. Lanes 1−3 are radioactively labeled in strand 1, and lanes 4−6 are radioactively labeled in strand 3. Lanes 1 and 4 contain just these single strands, but lanes 2 and 5 contain H2 SIJ3K complexes labeled in these strands. Lanes 3 and 6 contain the products, respectively, of treating the material in lanes 2 and 5 with VTopo I. The products are visible as a band of slower mobility. The system remains intact following treatment with the enzyme.

been recorded for all 10 of the SIJ3K variants shown in Figure 3. Lanes 1−3 of Figure 7 have been labeled in strand 1, and lanes 4−6 have been labeled in strand 3. Lanes 1 and 4 contain strands 1 and 3, respectively. Lanes 2 and 5 contain the substrate complex, before reaction, and lanes 3 and 6 contain the products of treating the substrates with VTopo I. It is clear in both cases that a new product with decreased mobility has resulted from treatment with VTopo I. Note that there is no apparent difference between the products in lanes 3 and 6. It is also evident that treatment by VTopo I does not lead to dissociation of the SIJ3K molecule.

Figure 8 illustrates denaturing gels that chart the progress of the reaction for the H2 SIJ3K molecule. Figure 8a contains the products of treating the molecule labeled in CCCTT-containing strand 1, which is transformed from a 69-mer (S) to a 62-nucleotide product (P). The cluster of rapidly migrating ^{32}P-labeled strands denoted C in lanes 3−9 corresponds to the covalent DNA−enzyme intermediate that has been digested by proteinase K to yield DNA−peptide adducts. Figure 8b is analogous to Figure 8a, except that strand 3 is labeled. In this case, the recombination event increases the length of the labeled strand from 62 nucleotides to 69 nucleotides. Similar gels have been obtained for each of the other species examined. In each case, bands corresponding to a covalent intermediate have been observed in every lane except for the untreated control, confirming the involvement of the covalent species in the mechanism.

Preferred Site for Recombination. A key goal of this study has been to establish the site preferred by VTopo I on a

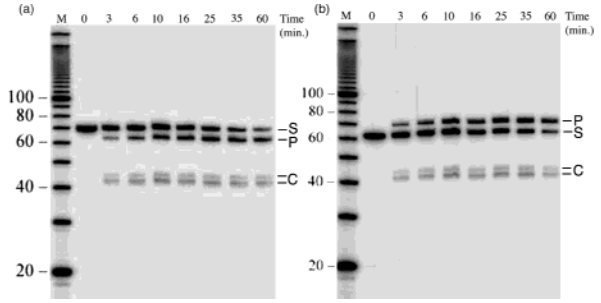

FIGURE 8: Time courses of the treatment of H2 SIJ3K molecules with *vaccinia* virus topoisomerase I. These are autoradiograms of denaturing 12% polyacrylamide gels. Strand 1 is labeled in panel a, and strand 3 is labeled in panel b. The reaction times are indicated above the lanes. The progress of the reaction in the molecule labeled on strand 1 in panel a may be monitored by following the conversion of a 69-mer substrate strand (labeled S) to a 62-mer product strand (labeled P); similarly, the progress of the reaction of in the molecule labeled on strand 3 in panel b may be monitored by following the conversion of a 62-mer substrate strand (S) to a 69-mer product strand (P). Two bands corresponding to the covalent intermediate digested with proteinase K (labeled C) are also visible in both panels. Lane M contains a 10-bp ladder. The sizes (in nt) of marker DNA strands are indicated on the left.

symmetric junction. We have scanned the available sites in an approach that proved successful with RuvC, although that study employed SIJ1K molecules (*16*). Holliday junctions are known to stack, so that there is a distinct crossover strand and a distinct noncrossover, or helical, strand (*40*). At the outset of this study, we did not know whether the preferred site was on the helical strand or on the crossover strand, so we have studied both possibilities. We have examined molecules with the scissile nucleotide at the junction and up to four nucleotides away from the junction. The molecules with the scissile nucleotide on the crossover strands are labeled C0···C4, and those with the scissile nucleotide on the helical strand are labeled H0···H4. We have quantitated the time course of the reaction for each of the species listed in Figure 3. It is important to remember that the difference between the C-series and the H-series is whether the crossover point lies on the same strand containing the scissile nucleotide, not whether VTopo I is cutting the same piece of double helix on the opposite strand. Thus, in the H-series experiments, the scissile site is on an edge of the rhombus, whereas in the C-series the scissile site is external to the rhombus.

The overall results are shown in Figure 9a, which illustrates that the H2 molecule is the substrate with both the highest initial velocity and the largest amount of product accumulated after 1 h. The C2 molecule is the second most effective substrate. The initial rates, extents of reaction, and strand biases (H/C ratios for rate and yield) are listed in Table 1. The strand biases are near unity for positions 2, 3, and 4. Positions 0 and 1 show very strong strand biases in favor of the scissile phosphodiester being on the helical strands.

The ratio of covalent topoisomerase−DNA intermediates to resolved product is plotted in Figure 9b. There is a qualitative relationship between the data in this plot and the reaction data in Figure 9a: the rank orders are approximately reversed so that the more reactive sites have lower ratios than the less reactive sites. These data bear on the rate limiting step but do not reveal it explicitly.

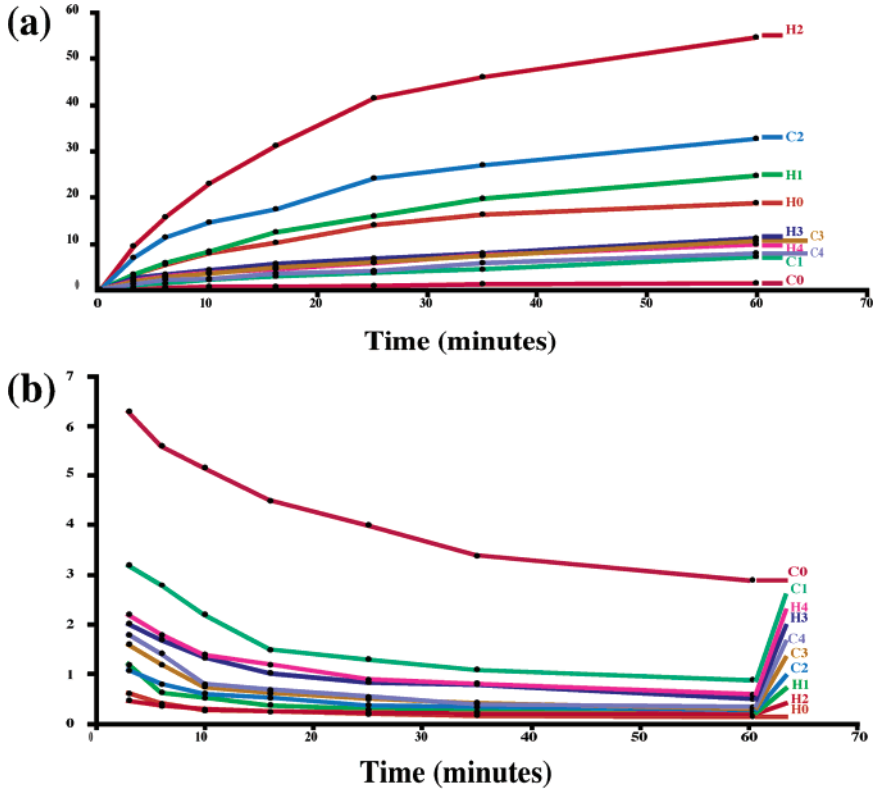

FIGURE 9: Comparison of time courses. (a) Reaction time courses. This plot compares the kinetics of the ten SIJ3K substrates used in these experiments. What is plotted is the level of the resolved recombinant molecule, not including the covalent intermediate. It is clear that the H2 complex is the best substrate, from the standpoints both of initial velocity and of accumulated product. (b) Ratios of covalent intermediates to products. The plot indicates the time course of the ratio of covalent intermediates to the products. The color coding is the same as in panel a; from the color coding, it is evident that the rank orderings are qualitatively reversed: the lower ratios are associated with the more reactive sites.

Table 1: Initial Rates of Resolution, Extents of Recombination, and Strand Bias at 60 Min

complex	C0	H0	C1	H1	C2	H2	C3	H3	C4	H4
initial rate (10^{-14} mol/min)	0.24	2.13	0.60	2.20	4.67	6.33	1.20	1.73	0.76	1.33
recombination extent at 60 min (%)	1.4	18.9	7.1	25.0	33.1	55.3	10.6	11.3	8.0	9.8
strand bias, ratio of H/C	13.50		3.52		1.67		1.13		1.23	
strand bias, H/C rate ratio	8.88		3.67		1.35		1.44		1.75	

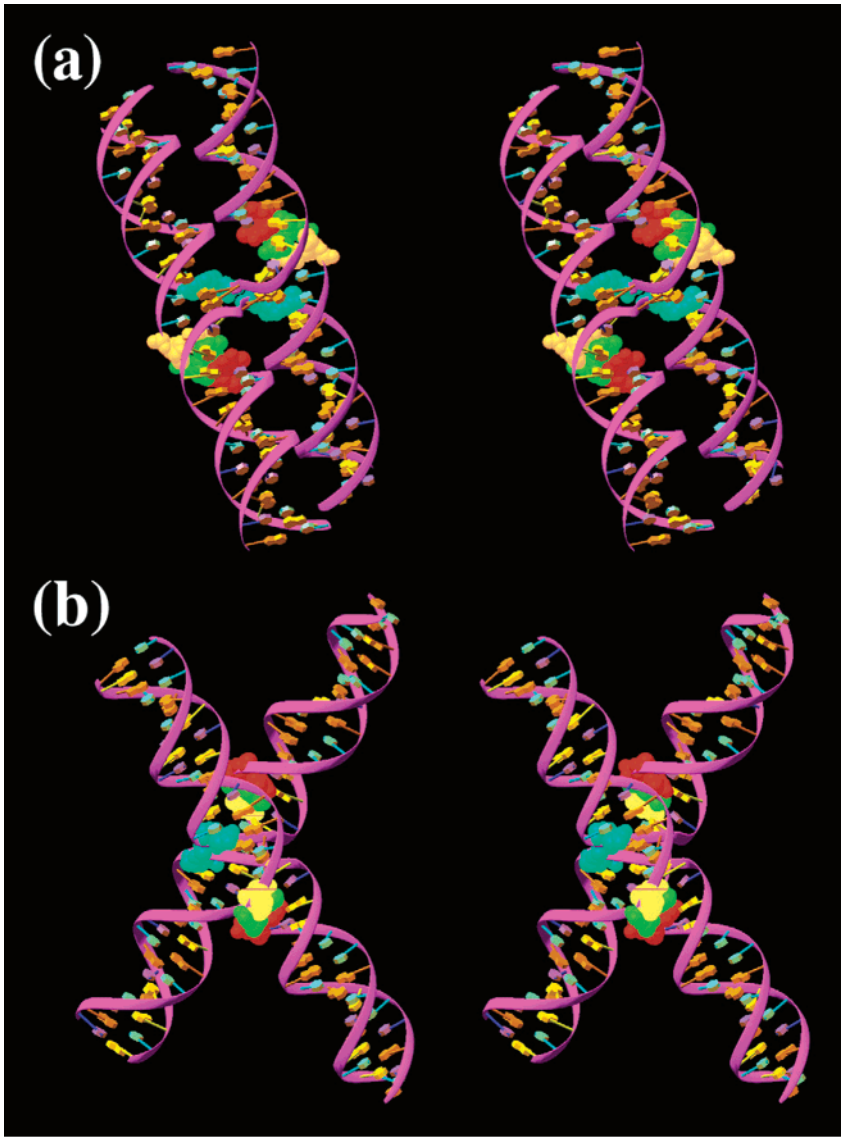

FIGURE 10: Stereoscopic three-dimensional structural models of the Holliday junction. The locations of the preferred cleavage sites are indicated on a simplified model of the Holliday junction; panel a is a view down the dyad axis, and panel b is a view with the dyad axis horizontal. Key nucleosides have been expanded to van der Waals models and then colored. The H2 positions are shown in red, H1 in green, H0 in orange, and C2 in turquoise. Although it is clear that the prominent H recombination sites are in similar locations, the environment of the C2 site appears to be quite different.

DISCUSSION

Symmetric Immobile Junctions of the Third Kind. The data presented here on the SIJ3K molecule demonstrate that we have been able to design and fabricate an undistorted symmetric immobile junction. We showed previously that the angle between the edges of a DNA parallelogram is a characteristic of the junction used and is affected by the junction-flanking sequence. As confirmed by atomic force microscopy, we have been able to observe different angles between edges for molecules with J1 junctions (*19*), Bowtie junctions (*25*), and symmetric junctions that contain the special sequence CCA (*31*); in each case, these results were consistent with expectations based on previous experiments. Thus, the SIJ3K molecule emulates the structure of an undistorted branched junction while preventing branch migration. The molecule with 1.5 turns per edge is the largest molecule that we were able to characterize as being an SIJ; hydroxyl radical autofootprinting revealed that the symmetric

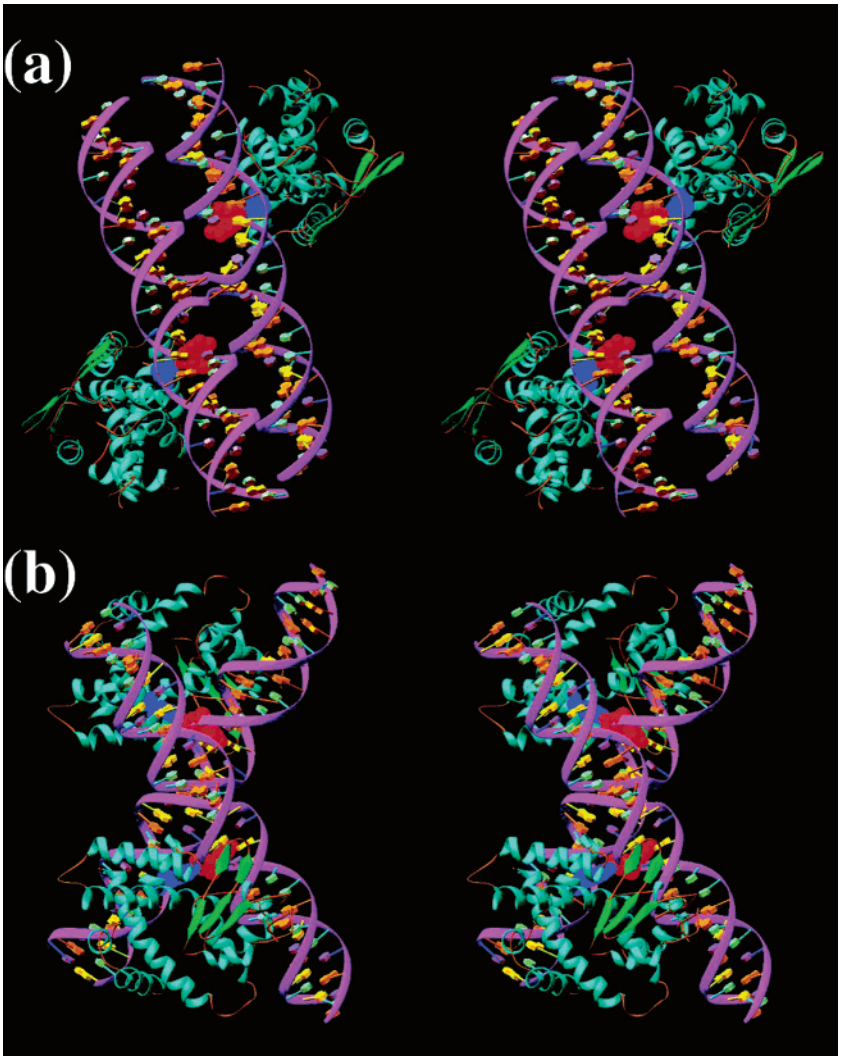

FIGURE 11: Stereoscopic three-dimensional structural models of the Holliday junction and its docking to the catalytic domain of *vaccinia* virus topoisomerase I. The catalytic domain has been docked into the molecule so as to juxtapose its catalytic tyrosine with the H2 reactive site. The views shown in panels a and b are those of Figures 10a,b, respectively.

junction in a candidate SIJ3K molecule with two turns per edge was not immobile (data not shown).

One key caveat involving the undistorted nature of the symmetric junction in a SIJ3K molecule is that some small amount of distortion could occur if the natural angle for the symmetric junction were to differ from the angles of the immobile junctions holding it fixed. The expectation is that this angle will not differ by more that 20° or so from the 63° angle of J1 immobile junctions; the unusual 43° angle seen in the case of CCA-containing junctions (*31*) can be attributed to a special hydrogen bond holding that junction in place (*20*). The distortions between the symmetric angle and the immobile angles may ultimately be minimized when data have been collected on the preferred angles for a variety of both immobile, and insofar as possible, symmetric junctions.

As noted previously, a number of thermodynamic (*13*, *14*) and enzymatic (*16*) studies have been performed with SIJ1K molecules. The flaws of SIJ1K were discussed earlier, both the unnatural constraint on the interdomain angle and the possible occlusion of enzymatic sites. It appears that it would be possible to use SIJ3K molecules to confirm or correct the conclusions drawn from those earlier studies. It is important to recognize that the dyad axis of the Holliday junction bisects the obtuse angle (*20*). Thus, cleavage experiments need only place the recognition site on a pair of helical or crossover strands flanking the obtuse angle, as shown in Figure 3. One cannot arrange symmetric sites to flank the acute angle.

Recombination of Holliday Junctions by Vaccinia Virus Topoisomerase I. Sekiguchi et al. (*36*) have demonstrated that there must be mobile nucleotides 3′ to the CCCTT recognition site of VTopoI. Thus, our search for the preferred site was limited to the 5′ side of the junction. We have demonstrated that the scissile site preferred by VTopo I is on the helical strands, two nucleotides 5′ to the junction. The hydroxyl radical characterization experiments present no evidence that any crossover isomerization (*7*) occurs in this system, so there is little reason to believe that the experiment is susceptible to problems involving this phenomenon.

Although it is clear that the H2 site is the preferred site, it is certainly not the only site at which topoisomerase can resolve the immobile junction. The C2, H1, and H0 systems all evince a significant level of activity. It is not hard to imagine that VTopo I could distort the structure of the

junction in the vicinity of the junction to make H1 and H0 resemble H2. Changing the angles between the helix axes of the four arms of the Holliday junction could be a natural component of the resolvase reaction, which mandates simultaneous binding and cleavage by two topoisomerase molecules at opposing CCCTT sites on the junction. The C2 site is on the other side of the junction, and its susceptibility is less readily explained by such arguments. The differences between the sites are evident in Figure 10a,b. This drawing shows junctions derived from the Eichman et al. (*20*) crystal structure, but modified to contain an expected 60° angle (*17*−*19*). Figure 11 shows a docking of the catalytic domain of the protein (*33*) to this Holliday junction in the H2 site. Binding of VTopo I to sites H2, H1, and H0 appears to occur on both symmetry-related DNA domains without any apparent interference between the two binding sites. However, binding to the C2 site can at best only take place at one site, resulting in blockage of the symmetry related site. The only way that the C2 site and the active H sites can be made equivalent is for the junction to be converted by VTopo I from the twisted antiparallel structure to something resembling the cruciform structure shown in Figure 2a. Within the context of a SIJ3K molecule, the site preferences may reflect the ease with which VTopo I can effect this transition from the various tested positions within the Holliday junction. We cannot exclude that cleavage at the first site may permit conformational flexibility that somehow exposes the second site.

Two mechanistic observations have been made regarding the reaction. The first is that the data show covalent enzyme adducts accompanying, and likely preceding, the appearance of products, confirming their role as intermediates in the recombination mechanism. The second is that the ratio of these intermediates to products is related qualitatively to the rate in an inverse fashion. These findings can be combined with the preference data and docking experiments via the suggestion that the covalent intermediates are not properly formed, or are formed on only one strand, in the least reactive sites, so that the reaction stalls there; this leads to an accumulation of intermediates and a paucity of products. In the absence of these structural arguments, one could conclude that the rate limiting step entails the rearrangements needed to produce the religated products. However, if all of the intermediates formed equally well, and the rate limiting step were the conversion from covalent intermediates to products, the positional effects noted here would likely not be so pronounced.

REFERENCES

1. Holliday, R. (1964) Mechanism for gene conversion in fungi, *Genet. Res. 5*, 282−304.
2. Hoess, R., Wierzbicki, A., and Abremski, K. (1987) Isolation and characterization of intermediates in site-specific recombination, *Proc. Natl. Acad. Sci. U.S.A. 84*, 6840−6844.
3. Kitts, P. A., and Nash, H. A. (1987) Homology-dependent interactions in phage-λ site-specific recombination, *Nature 329*, 346−348.
4. Nunes-Duby, S. E., Matsumoto, L., and Landy, A. (1987) Site-specific recombination intermediates trapped with suicide substrates, *Cell 50*, 779−788.
5. DasGupta, C., Wu, A. M., Kahn, R., Cunningham, R. P., and Radding, C. M. (1981) Concerted strand exchange and formation of Holliday structures by *Escherichia coli* RecA protein, *Cell 25*, 507−516.
6. Hsieh, P., and Panyutin, I. G. (1995) DNA branch migration, *Nucleic Acids & Mol. Biol. 9* (Eckstein, F., and Lilley, D. M. J., Eds.) pp 42−65, Springer-Verlag, Berlin.
7. Li, X., Wang, H., and Seeman, N. C. (1997) Direct evidence for Holliday junction crossover isomerization, *Biochemistry 36*, 4240−4247.
8. Mueller, J. E., Kemper, B., Cunningham, R. P., Kallenbach, N. R., and Seeman, N. C. (1988) T4 endonuclease VII cleaves the crossover strands of Holliday junction analogues, *Proc. Natl. Acad. Sci. U.S.A. 85*, 9441−9445.
9. Shinagawa, H., and Iwasaki, H. (1996) Processing the Holliday junction in homologous recombination, *Trends Biochem. Sci. 21*, 107−111.
10. Sekiguchi, J. A., Seeman, N. C., and Shuman, S. (1996) Asymmetric resolution of Holliday junctions by eukaryotic DNA topoisomerase I, *Proc. Natl. Acad. Sci. U.S.A. 93*, 785−789.
11. Zhang, S., Fu, T.-J., and Seeman, N. C. (1993) Construction of symmetric, immobile DNA branched junctions, *Biochemistry 32*, 8062−8067.
12. Fu, T.-J., and Seeman, N. C. (1993) DNA double crossover structures, *Biochemistry 32*, 3211−3220.
13. Zhang, S., and Seeman, N. C. (1994) Symmetric Holliday junction crossover isomers, *J. Mol. Biol. 238*, 658−668.
14. Sun, W., Mao, C., Liu, F., and Seeman, N. C. (1998) Sequence dependence of branch migratory minima, *J. Mol. Biol. 282*, 59−70.
15. Sha, R., Liu, F., and Seeman, N. C. (2000) Direct evidence for spontaneous branch migration in antiparallel DNA Holliday junctions, *Biochemistry 39*, 11514−11522.
16. Sha, R., Iwasaki, H., Liu, F., Shinagawa, H., and Seeman, N. C. (2000) Cleavage of symmetric immobile DNA junctions by *Escherichia coli RuvC*, *Biochemistry 39*, 11982−11988.
17. Murchie, A. I. H., Clegg, R. M., von Kitzing, E., Duckett, D. R., Diekmann, S., and Lilley, D. M. J. (1989) Fluorescence energy-transfer shows that the four-way DNA junction is a right-handed cross of antiparallel molecules, *Nature 341*, 763−766.
18. Eis, P., and Millar, D. P. (1993) Conformational distributions of a four-way DNA junction revealed by time-resolved fluorescence resonance energy-transfer, *Biochemistry 32*, 13852−13860.
19. Mao, C., Sun, W., and Seeman, N. C. (1999) Designed two-dimensional DNA Holliday junction arrays visualized by atomic force microscopy, *J. Am. Chem. Soc. 121*, 5437−5443.
20. Eichman, B. F., Vargason, J. M., Mooers, B. H. M., and Ho, P. S. (2000) The Holliday junction in an inverted repeat DNA sequence: sequence effects on the structure of four-way junctions, *Proc. Natl. Acad. Sci. U.S.A. 97*, 3971−3976.
21. Li, X., Yang, X., Qi, J., and Seeman, N. C. (1996) Antiparallel DNA double crossover molecules as components for nanoconstruction, *J. Am. Chem. Soc. 118*, 6131−6140.
22. Sa-Ardyen, P., Vologodskii, A. V., and Seeman, N. C. (2003) The flexibility of DNA double crossover molecules, *Biophys. J. 84*, 3829−3837.
23. Sha, R., Liu, F., Iwasaki, H., and Seeman, N. C. (2002) Parallel symmetric immobile DNA junctions as substrates for *Escerichia coli* RuvC Holliday junction resolvase, *Biochemistry 41*, 10985−10993.
24. Sha, R., Liu, F., Bruist, M. F., and Seeman, N. C. (1999) Parallel helical domains in DNA branched junctions containing 5′,5′ and 3′,3′ linkages, *Biochemistry 38*, 2832−2841.
25. Sha, R., Liu, F. Millar, D. P., and Seeman, N. C. (2000) Atomic force microscopy of parallel DNA branched junction arrays, *Chem. Biol. 7*, 743−751.
26. Rentzeperis, D., Rippe, K., Jovin, T. M., and Marky, L. A. (1992) Calorimetric characterization of parallel-stranded DNA stability, conformational flexibility, and ion binding, *J. Am. Chem. Soc. 114*, 5926−5928.
27. Lilley, D. M. J., and Clegg, R. M. (1993) The structure of the four-way junction in DNA, *Annu. Rev. Biophys. Biomol. Struct. 22*, 299−328.
28. Seeman, N. C., and Kallenbach, N. R. (1994) DNA branched junctions, *Annu. Rev. Biophys. Biomol. Struct. 23*, 53−86.
29. Carbone, A., and Seeman, N. C. (2002) Fractal designs based on DNA parallelogram structures, *Nat. Comput. 1*, 469−480.
30. Carbone, A., and Seeman, N. C. (2003) Coding and geometrical shapes in nanostructures: a fractal DNA-assembly, *Nat. Comput. 2*, 133−151.
31. Sha, R., Liu, F., and Seeman, N. C. (2002) Atomic force measurement of the interdomain angle in symmetric Holliday junctions, *Biochemistry 41*, 5950−5955.

32. Shuman, S., and Prescott, J. (1990) Specific DNA cleavage and binding by *vaccinia* virus-DNA topoisomerase I, *J. Biol. Chem. 265*, 17826−17836.
33. Cheng, C., Kussie, P., Pavletich, N., and Shuman, S. (1998) Conservation of structure and mechanism between eukaryotic topoisomerase I and site-specific recombinases, *Cell 92*, 841−850.
34. Van Duyne, G. D. (2001) A structural view of Cre-loxP site-specific recombination, *Annu. Rev. Biophys. Biomol. Struct. 30*, 87−104.
35. Guo, F., Gopaul, D. N., and van Duyne, G. D. (1997) Structure of Cre recombinase complexed with DNA in a site-specific recombination synapse, *Nature 389*, 40−46.
36. Sekiguchi, J., Cheng, C., and Shuman, S. (2000) Resolution of a Holliday junction by *vaccinia* topoisomerase requires a spacer DNA segment 3′ of the CCCTT down arrow cleavage sites, *Nucl. Acids Res. 28*, 2658−2663.
37. Caruthers, M. H. (1985) Gene synthesis machines: DNA chemistry and its uses, *Science 230*, 281−285.
38. Maxam, A. M., and Gilbert, W. (1977) New method for sequencing DNA, *Proc. Natl. Acad. Sci. U.S.A. 74*, 560−564.
39. Tullius, T. D., and Dombroski, B. (1985) Iron(II) EDTA used to measure the helical twist along any DNA molecule, *Science 230*, 679−681.
40. Churchill, M. E. A., Tullius, T. D., Kallenbach, N. R., and Seeman, N. C. (1988) A Holliday recombination intermediate is 2-fold symmetric, *Proc. Natl. Acad. Sci. U.S.A. 85*, 4653−4656.
41. Shuman, S. (1989) *Vaccinia* DNA topoisomerase-I promotes illegitimate recombination in *Escherichia coli*, *Proc. Natl. Acad. Sci. U.S.A. 86*, 3489−3493.
42. Roussel, A., and Cambillau, C. (1991) Turbo-Frodo, in *Silicon Graphics Directory*, Silicon Graphics, Mountain View, CA.
43. Carson, M. (1997) in *Ribbons* (Sweet, R. M., and Carter, C. W., Eds.) *Methods in Enzymology*, Vol. 277, pp 493−505, Academic Press, San Diego.
44. Seeman, N. C., and Kallenbach, N. R. (1983) Design of immobile nucleic acid junctions, *Biophys. J. 44*, 201−209.
45. Kallenbach, N. R., Ma, R.-I., and Seeman, N. C. (1983) An immobile nucleic acid junction constructed from oligonucleotides, *Nature (London) 305*, 829−831.
46. Seeman, N. C. (1990) De novo design of sequences for nucleic acid structure engineering, *J. Biomol. Struct. Dyn. 8*, 573−581.
47. Seeman, N. C. (2002) Key experimental approaches in DNA nanotechnology, in *Current Protocols in Nucleic Acid Chemistry*, Unit 12.1, John Wiley & Sons, New York.

BI0358061